



## Pressure-enhanced activity and stability of $\alpha$ -L-rhamnosidase and $\beta$ -D-glucosidase activities expressed by naringinase

Helder Vila-Real<sup>a</sup>, António J. Alfaia<sup>a</sup>, Robert S. Phillips<sup>b,c</sup>, António R. Calado<sup>a</sup>, Maria H.L. Ribeiro<sup>a,\*</sup>

<sup>a</sup> Faculdade Farmácia, Research Institute for Medicines and Pharmaceutical Sciences (i-Med-UL), University of Lisbon, Av. Prof. Gama Pinto, 1649-003 Lisbon, Portugal

<sup>b</sup> Department of Chemistry, University of Georgia, Athens, GA 30602, USA

<sup>c</sup> Department of Biochemistry and Molecular Biology, University of Georgia, Athens, GA 30602, USA

### ARTICLE INFO

#### Article history:

Available online 1 February 2010

#### Keywords:

$\alpha$ -L-Rhamnosidase  
 $\beta$ -D-Glucosidase  
 Naringinase  
 High pressure  
 Reaction volume  
 Activation volume

### ABSTRACT

Naringinase is an enzyme complex, expressing  $\alpha$ -L-rhamnosidase and  $\beta$ -D-glucosidase activities. The impact of high pressure and temperature on naringinase activity and stability were studied, in order to assess the potential of enzyme thermostability on glycosides hydrolyses. To a better understanding of these effects on naringinase enzyme complex, they were also evaluated over  $\alpha$ -L-rhamnosidase and  $\beta$ -D-glucosidase activities, using specific substrates, p-nitrophenyl  $\alpha$ -L-rhamnopyranoside (4-NRham) and p-nitrophenyl  $\beta$ -D-glucopyranoside (4-NGLuc), respectively. Hydrolysis rate of 4-NRham and naringin increased with pressure from 0.1 to 150 MPa.

The equilibrium constants for  $\alpha$ -L-rhamnosidase and  $\beta$ -D-glucosidase reactions, at pressures of 0.1–200 MPa and 40 °C, were determined and best fitted with the model of Baliga and Whalley equation. Accordingly, reaction volumes of 93 and 64 mL mol<sup>-1</sup> were obtained for  $\alpha$ -L-rhamnosidase and  $\beta$ -D-glucosidase reactions, respectively. Reaction rate constants were also determined at the same experimental conditions and well fitted to the models of Golinkin, Laidlaw, Hynes and of Burris and Laidler. A negative  $\Delta V^\ddagger$  of  $-7.7 \pm 1.5$  and  $-20.0 \pm 5.2$  mL mol<sup>-1</sup> were obtained for  $\alpha$ -L-rhamnosidase and naringinase reactions, correspondingly, which reflect the accelerating effect of pressure on the biocatalysis.

Moreover, the  $K_M$ ,  $k_{cat}$  and  $k_{cat}/K_M$  values, on naringin hydrolysis under atmospheric (0.1 MPa) and high pressure (150 MPa) conditions at different temperatures (25–80 °C) were determined. A 3-fold and 4-fold increase on naringinase thermostability was observed under 150 MPa at 70 and 80 °C, respectively, compared to 0.1 MPa experiments. In addition, a 15-fold increase of  $k_{cat}/K_M$  values from experimental conditions of 0.1 MPa and 30 °C to 150 MPa and 70 °C was observed. In fact, high pressure showed to be a powerful tool to increase stability of naringinase against thermal denaturation. In conclusion, the effect of amplification of pressure effects on reaction rates by temperature could have a pragmatic use for accelerating enzymatic reactions.

© 2010 Elsevier B.V. All rights reserved.

### 1. Introduction

Biocatalysis is reaching a key position in drug development, driving to new opportunities and being able to create new synthetic routes [1]. In fact, the functional dependencies of biocatalysts activity, namely pH, temperature, solvent and pressure [2–4], alone or combined, can be used to modulate it, in order to attain improved results.

In this context, recent results showed that all the potentialities of high pressure, have not yet been explored [5]. Pressure can change both enzyme stability and activity or even give information on the protein structure [6]. Several strategies, beyond enzyme genetic modification, have been employed to enhance the enzyme

activity, stability and re-usage capacity, including: immobilization, use of non-aqueous media, among others. High pressure may be a complementary, synergistic, or an additive enzyme improvement technique. Moreover, the ability of control simultaneously pressure and temperature, can significantly enhance the capacity to adjust the same enzymatic system to different substrates or to gain activity toward diverse final products.

Pressure has been used to shift chemical equilibria or even to accelerate processes according to the Le Chatelier's principle as well as to the transition state theory. Depending on pressure magnitude, it is able to interfere with secondary, tertiary and quaternary structure of proteins [7]. The enzyme native state is dependent on temperature and pressure, drawing an elliptical phase diagram of protein denaturing, which shows an interesting behavior for modulating protein stability. Considering the diagram of Fig. 1, at low pressure range proteins will denature at lower temperatures [8]. In the opposite situation, higher pressures will avoid thermal protein

\* Corresponding author. Tel.: +351 21 7946400; fax: +351 21 7946470.  
 E-mail address: [mhribeiro@ff.ul.pt](mailto:mhribeiro@ff.ul.pt) (M.H.L. Ribeiro).

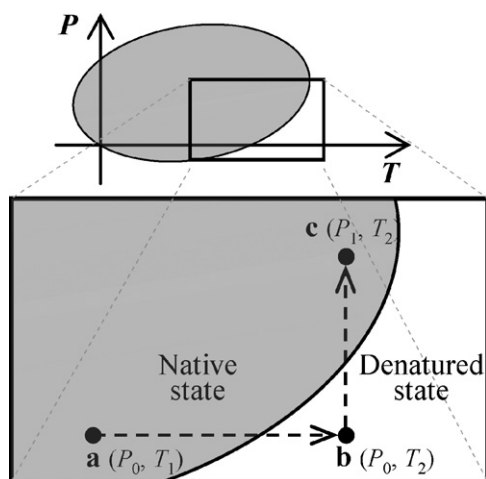


**Fig. 1.** Elliptical phase protein denaturing diagram. From **a** to **b** temperature increases and protein starts to denaturate but if pressure is raised till **c** protein native state is preserved.

denaturation at high temperatures, which may favour the enzyme native state [8].

A thermodynamic insight to the phenomenon directs us to the lead responsibility of the volumetric changes, along the reaction coordinate, on the catalytic expression of an enzyme [9]. In fact, the conformational adjustments between the biocatalyst and the substrate in concert with the breakdown and/or formation of chemical bonds, as affected by pressure and temperature variations, can considerably change the overcoming of the energetic barrier to attain the transition state and later on the reaction products. Nevertheless, this becomes more difficult to fully understand when the enzymatic system has multiple activities. This is true for the naringinase enzyme complex, obtained from *Penicillium decumbens*, expressing  $\alpha$ -L-rhamnosidase and  $\beta$ -D-glucosidase activities. Naringinase is of relevance in food and pharmaceutical industries. Naringin can be hydrolyzed by  $\alpha$ -L-rhamnosidase activity of naringinase to rhamnose and prunin, which can be further hydrolyzed by the  $\beta$ -D-glucosidase component of naringinase into glucose and tasteless naringenin [10] (Fig. 2). The relevance of these molecules to the industrial sector is due to their recognized antioxidant, anti-inflammatory [11,12], antiulcer, and hypocholesterolemic effects, whereas naringenin has also shown antimutagenic and neuroprotective activities and prunin antiviral activity. Both naringin and naringenin have similar medical applications, suggesting that the biological activity is not associated with the sugar residues but is rather related to the aglycon moiety.

In this work is our aim to study the combined effect of pressure and temperature over equilibrium and reaction rate constants of both  $\alpha$ -L-rhamnosidase and  $\beta$ -D-glucosidase expressed by naringinase enzyme complex. For this purpose and in order to discriminate both catalytic activities two specific substrates were used: 4-nitrophenyl- $\alpha$ -L-rhamnopyranoside (4-NGluc) and 4-nitrophenyl- $\beta$ -D-glucopyranoside (4-NRham). As naringin solubility increased with temperature a higher productivity is expected if the enzyme does not denatured. Therefore the impact of high pressure and temperature on naringinase catalytic activity and stability was carried out, accessing the protective effect of high pressure on enzyme thermostability.

## 2. Theory

Transition state theory (TST) is commonly used as a qualitative basis to achieve mechanistic information on chemical reactions [13]. Although, the physical and chemical details of the mecha-

nisms by which enzymes catalyze chemical reactions are still a matter of some controversy, accurate experimental data on rate constants can be used to successfully calculate thermodynamic functions of activation (TFA) and show some insights on catalysis, at a macroscopic level, which was one of the aims of this work.

### 2.1. Temperature effect

Regarding to TST formulation, reaction rate constant ( $k$ ) is related to the standard Gibbs energy of activation ( $\Delta G^\ddagger$ ) by the following equation:

$$k = \frac{k_B T}{h} e^{-\Delta G^\ddagger / RT} \quad (1)$$

where  $k_B$  is the Boltzmann constant ( $1.38 \times 10^{-23} \text{ J K}^{-1}$ ),  $h$  is the Planck constant ( $6.63 \times 10^{-34} \text{ J s}$ ),  $R$  is the gas constant ( $8.314 \text{ J K}^{-1} \text{ mol}^{-1}$ ) and  $T$  is the absolute temperature (K).

Moreover, it is a well known experimental fact that  $k$  is temperature dependent, and the empirical Arrhenius equation still constitute the main mathematical relation used to describe it. This equation, a first order polynomial describing  $\ln k$  as function of  $T^{-1}$ , can be rewrite as:

$$\ln k = A + \frac{B}{T} \quad (2)$$

where  $A$  and  $B$  are empirical parameters related to TFA, according to Eq. (5).

Nevertheless, in case of enzymatic catalysis, often is found that the former relation frequently does not fit satisfactorily to experimental data, probably because the proteins are not rigid structures [14]. In fact, an innovative approach can be considering the second order polynomial relation known as the Wold and Ahlberg equation [15] to achieve TFA values. In this equation  $C$  is an empirical parameter.

$$\ln k = A + \frac{B}{T} + \frac{C}{T^2} \quad (3)$$

### 2.2. Pressure effect

In line with the previous assumptions, pressure effects on equilibrium ( $K$ ) and rate constants ( $k$ ) were initially quantified according to the best fit of experimental data to first and second order polynomials relating  $\ln K$  or  $\ln k$  to  $P$  [Eqs. (4) and (5)]:

$$\ln K = A + BP \quad \text{or} \quad \ln k = A + BP \quad (4)$$

$$\ln K = A + BP + CP^2 \quad \text{or} \quad \ln k = A + BP + CP^2 \quad (5)$$

According to these equations, known as Burris and Laidler [16] and Golinkin, Laidlaw and Hyne [17] equations, respectively volumetric changes along reaction coordinate may be achieved.

Actually, from  $\ln K$  dependence we estimated the reaction volumes ( $\Delta V_{\text{Reac}}$ ) and from  $\ln k$  dependence on pressure we can calculate activation volumes ( $\Delta V^\ddagger$ ). Moreover, the slope resulting from fitting Eq. (4) to experimental data is equal to  $\Delta V_{\text{Reac}}/RT$  or  $-\Delta V^\ddagger/RT$ , and from Eq. (5) adjustment both volumetric changes ( $\Delta V$ ) are given as:

$$\Delta V = -RT(B + 2CP) \quad (6)$$

Additionally, Eq. (7), Baliga and Whalley [18] and the third order polynomial Eq. (8), Walling and Tanner [19] were also considered.

$$\ln K = \frac{A + BP}{1 + CP} \quad \text{or} \quad \ln k = \frac{A + BP}{1 + CP} \quad (7)$$

$$\ln K = A + BP + CP^2 + DP^3 \quad \text{or} \quad \ln k = A + BP + CP^2 + DP^3 \quad (8)$$

Following the assumption taken to calculate volumetric changes with the first and second order polynomials fits, for Walling and Tanner equation we used:

$$\Delta V = -RT(B + 2CP + 3DP^2) \quad (9)$$

Likewise, reaction and activation volumes calculated according to the fit of data to the relation proposed by Baliga and Whalley [Eq. (7)] drive to Eq. (10):

$$\Delta V = -RT \frac{(B - AC)}{(1 + CP)^2} \quad (10)$$

### 2.3. Standard thermodynamic parameters

The standard thermodynamic parameters for the enzyme–substrate complex formation were studied using the specific laws. Standard Gibbs energy,  $\Delta G^\circ$ , was calculated from Eq. (11):

$$\Delta G^\circ = -RT \ln K \quad (11)$$

( $K$ , enzyme–substrate complex equilibrium constant;  $\Delta G^\circ$ , enzyme–substrate complex formation standard Gibbs energy)

Standard enthalpy,  $\Delta H^\circ$ , as well as standard entropy,  $\Delta S^\circ$ , was determined using Eq. (12). The enthalpy parameter was taken from the linear regression slope, while standard entropy is equal to y-intercept [Eq. (13)]:

$$d\left(\frac{\Delta G^\circ}{T}\right) = \Delta H^\circ d\left(\frac{1}{T}\right) \quad (12)$$

$$\frac{\Delta G^\circ}{T} = -\Delta S^\circ + \frac{\Delta H^\circ}{T} \quad (13)$$

### 2.4. Thermodynamic functions of activation

Considering an Arrhenius behavior of  $k_{\text{cat}}$  data over temperature, the activation energy,  $E_a$ , was assessed from the slope of  $k_{\text{cat}}$  against  $T^{-1}$  re-writing Eq. (2) into the next form:

$$\ln k_{\text{cat}} = \ln A - \frac{E_a}{R} T^{-1} \quad (14)$$

Activation enthalpy ( $\Delta H^\ddagger$ ), activation entropy ( $\Delta S^\ddagger$ ) and activation Gibbs energy ( $\Delta G^\ddagger$ ) were determined according to the correspondent equation adopted. For the Arrhenius fit, and taking into account the thermodynamic fundamental equation:

$$\Delta G^\ddagger = \Delta H^\ddagger - T\Delta S^\ddagger \quad (15)$$

the activation enthalpy ( $\Delta H^\ddagger$ ) can be derived from the slope of the linear regression  $\ln k$  versus  $1/T$ , while activation entropy ( $\Delta S^\ddagger$ ) could be calculated from y intersection, according to:

$$\ln k = \ln \frac{k_B T}{h} + \frac{\Delta S^\ddagger}{R} - \frac{\Delta H^\ddagger}{RT} \quad (16)$$

With respect of Wold and Ahlberg model [15], and considering both Eq. (3) and TST,  $\Delta H^\ddagger$  and  $\Delta S^\ddagger$  were determined, respectively, from the kinetic data by the expressions:

$$\Delta H^\ddagger = -R \left( B + \frac{2C}{T} + T \right) \quad (17)$$

$$\Delta S^\ddagger = R \left[ \ln \left( \frac{h}{k_B} \right) + A - 1 - \frac{C}{T^2} - \ln T \right] \quad (18)$$

Activation Gibbs energy ( $\Delta G^\ddagger$ ) can be calculated after  $\Delta H^\ddagger$  and  $\Delta S^\ddagger$ , using Eq. (4) or directly from the  $k$  value through Eq. (11).

$$\Delta G^\ddagger = RT \left( \ln \frac{k_B T}{h} - \ln k \right) \quad (19)$$

## 3. Materials and methods

### 3.1. Materials

Naringin, p-nitrophenyl  $\alpha$ -L-rhamnopyranoside, p-nitrophenyl  $\beta$ -D-glucopyranoside were from Sigma–Aldrich. All other chemicals were analytical grade and obtained from various sources.

### 3.2. Enzyme solution

Naringinase (CAS no. 9068-31-9, cat. no. 1385) from *P. decumbens* was obtained from Sigma–Aldrich and stored at  $-20^\circ\text{C}$ . The lyophilized naringinase powder was dissolved in 20.0 mM acetate buffer pH 4.0, at 200 mg mL $^{-1}$  concentration. The enzyme solution was kept at  $4^\circ\text{C}$ .

### 3.3. Analytical methods

In this work reducing sugars were determined using the DNS macroassay [20] modified into a microassay procedure using a microtiter plate. Absorbance was read at 575 nm. The reducing sugars concentration was determined against a glucose calibration curve.

The protein content was determined using Bradford assay from Bio-Rad protein microassay procedure, using a naringinase calibration curve [21].

The concentration of the flavanones, naringin and naringenin, was determined through the absorbance measured at 280 nm, using a calibration curve of each flavanone.

The concentration of p-nitrophenyl  $\alpha$ -L-rhamnopyranoside and p-nitrophenyl  $\beta$ -D-glucopyranoside was evaluated spectrophotometrically (Zenith 3100 spectrofluorimeter) at  $\lambda = 340$  nm, using a calibration curve of each compound.

### 3.4. Activity measurement

To evaluate  $\alpha$ -L-rhamnosidase activity expressed by naringinase, p-nitrophenyl  $\alpha$ -L-rhamnopyranoside (4-NRham) at 0.40 mM concentration in 20.0 mM acetate buffer pH 4.0 was used as substrate while p-nitrophenyl  $\beta$ -D-glucopyranoside (4-NGLuc) at equal concentration was used as substrate on  $\beta$ -D-glucosidase activity determination.

The enzymatic hydrolysis of the substrates p-nitrophenyl  $\alpha$ -L-rhamnopyranoside and p-nitrophenyl  $\beta$ -D-glucopyranoside was followed through absorption measured at 340 nm every 30 s during 10 min,  $30.0^\circ\text{C}$ , at atmospheric pressure. In both reactions 1 mol of substrate led to 1 mol of product. A calibration curve was built for each substrate and respective product. The enzyme activity ( $A$ ) of  $\alpha$ -L-rhamnosidase and  $\beta$ -D-glucosidase expressed by naringinase was calculated by linear regression on the first data-points during the initial 30 min reaction time.

Naringin bioconversion studies were carried out in standard solutions of naringin in acetate buffer (20.0 mM), at pH 4.0 and at atmospheric pressure (0.1 MPa), as well as, under high pressure (150 MPa).

Kinetic measurements at atmospheric pressure were performed, in triplicate, using a continuous sampling method along the catalytic reaction. In the high pressure catalytic reaction studies, each data point, obtained in triplicate, required a new experiment due to the depressurization needed at the end of the incubation period. The reaction media was set in polyethylene bags pressurized in a high pressure vessel [10]. Pressure was raised following a standard procedure in a way to avoid reaction overheating. Subsequently, the pressure was released within 1 min; the reaction was immediately stopped, lowering the temperature of solutions below  $0^\circ\text{C}$  and the samples were frozen ( $-20^\circ\text{C}$ ) until the enzy-

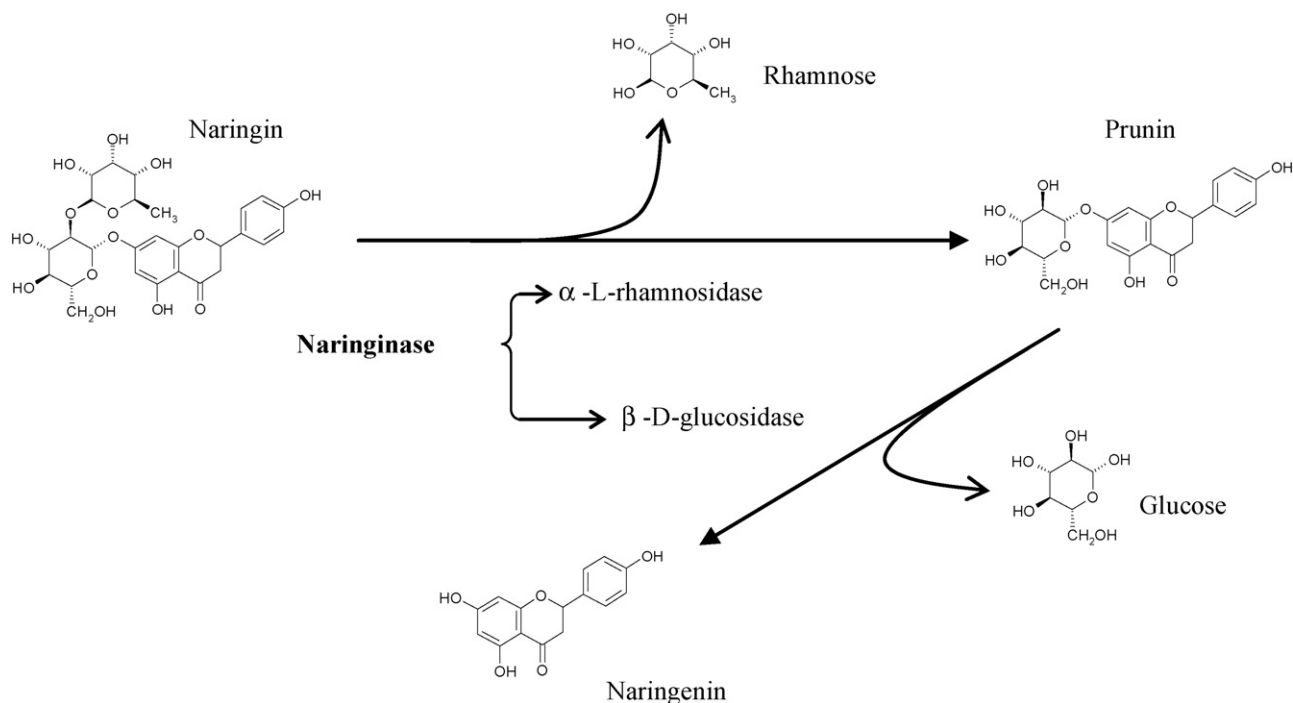


Fig. 2. Hydrolysis of naringin into prunin, rhamnose, naringenin and glucose by naringinase expressing  $\alpha$ -L-rhamnosidase and  $\beta$ -D-glucosidase activities.

matic activity assays were carried out. The pressure dependence fitted to experimental data of equilibrium constants and reaction rate constants were carried out using the same non-linear curve-fit program Excel for Windows, version 8.0 SR2.

Kinetic measurements at different temperatures on naringinase activity ranged from 25.0 to 80.0 °C. The naringinase concentrations ranged from 5 to 75 mg mL<sup>-1</sup>, according to the experimental temperature, in order to obtain a straight linear progression during the first 80 min. The temperature dependence of experimental data to the Arrhenius equation model was carried out using the same non-linear curve-fit program Excel for Windows, version 8.0 SR2.

Naringinase activity was calculated, by linear regression on the first linear data-points, from the slopes of the plot of reducing sugars concentration *versus* time. The fit of the Michaelis–Menten model:  $V = [S] V_{\max} / ([S] + K_M)$  ( $V$ , initial reaction rate;  $[S]$ , substrate concentration;  $V_{\max}$ , maximum initial rate;  $K_M$ , Michaelis–Menten constant) to experimental data was carried out using a non-linear curve-fit program in Excel for Windows, version 8.0 SR2, by minimizing the residual sum of squares between the experimental data-points and the estimated values by the model. The kinetic parameters estimated by Lineweaver–Burk linear regression were used as initial values of this non-linear curve-fit program. Following this methodology, the catalytic constants,  $k_{\text{cat}}$ , were determined according to:  $k_{\text{cat}} = V_{\max} / [E_t]$  ( $k_{\text{cat}}$ , catalytic constant;  $V_{\max}$ , maximum initial reaction rate;  $[E_t]$ , total enzyme concentration)

## 4. Results and discussion

### 4.1. Effect of pressure on $\alpha$ -L-rhamnosidase and $\beta$ -D-glucosidase activities of naringinase

The effect of pressure, from 0.1 (atmospheric pressure) to 200 MPa, at 40 °C, was assessed for both  $\beta$ -D-glucosidase and  $\alpha$ -L-rhamnosidase activities expressed by naringinase. These experiments allowed the determination of equilibrium constants and reaction volume as well reaction rate constants and

the activation volumes for both enzymatic reactions as shown below.

#### 4.1.1. Equilibrium constant and reaction volume determination

Fig. 3 shows the dependence of pressure on equilibrium constants ( $K$ ) of the specific substrates 4-NRham and 4-NGluc hydrolysed by  $\alpha$ -L-rhamnosidase and  $\beta$ -D-glucosidase expressed by naringinase. Lower equilibrium constants of both substrates were obtained as pressure increased. When  $\ln K$  was plotted against pressure according to Eq. (4), two curved lines with similar decreasing slopes, were obtained (Fig. 3).

Pressure effects on equilibrium constants ( $K$ ) were quantified fitting the experimental data to first and third order polynomials, respectively described by the models of Baliga and Whalley (Eq.

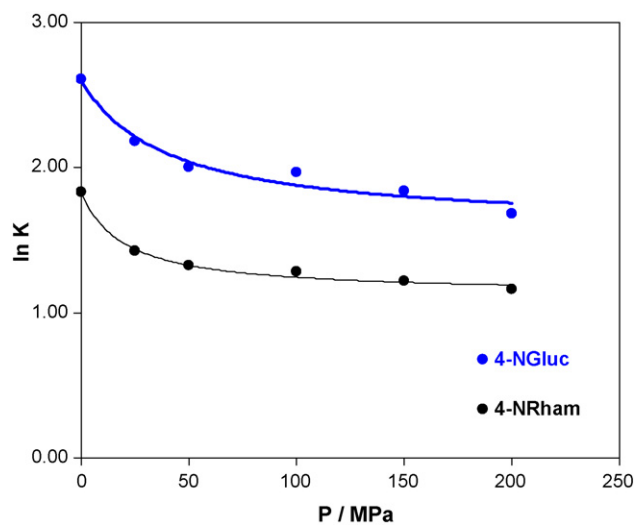


Fig. 3. Equilibrium constant pressure dependence for the hydrolysis of 4-NGluc and 4-NRham by  $\alpha$ -L-rhamnosidase and  $\beta$ -D-glucosidase of naringinase, in acetate buffer pH=4.0,  $T=40$  °C (mean value,  $n=3$ ).

**Table 1**  
Reaction volume estimation, for the hydrolysis of 4-NGLuc and 4-NRham by naringinase ( $T=40^\circ\text{C}$ ) (mean value  $\pm$  standard deviation,  $n=3$ ).

| Models                               | 4-NGLuc |       | $\Delta V_{\text{Reac}}$ (mL mol $^{-1}$ ) | 4-NRham |       | $\Delta V_{\text{Reac}}$ (mL mol $^{-1}$ ) |
|--------------------------------------|---------|-------|--|---------|-------|--|
|                                      | F-test  |       |  | F-test  |       |  |
|                                      | $f$     | $f_c$ |  | $f$     | $f_c$ |  |
| Golinkin, Laidlaw and Hyne (Eq. (5)) | 2.1     | 10.1  | –  | 3.5     | 10.1  | –  |
| Walling and Tanner (Eq. (8))         | 8.9     | 19    | –  | 8.0     | 19    | –  |
| Whalley and Baliga (Eq. (7))         | 14.3    | 10.1  | 64.3                                       | 113.0   | 10.1  | 93.1                                       |

$$f = ((SSE_1 - SSE_2)/(q_2 - q_1))/(SSE_2/(n - q_2)) (95\%).$$

$$f_c = (p_2 - p_1, n - p_2).$$

$n$ , experimental points;  $q$ , number of parameters; SSE, sum of square residues.

(7)) [18], Golinkin, Laidlaw and Hyne (Eq. (5)) [17] and Walling and Tanner (Eq. (8)) [19]. The  $F$ -test (Fisher-Snedecor test) (Table 1) was used to choose the model that fitted better the experimental results. In fact, Baliga and Whalley model [18] was the best to fit the equilibrium constant pressure and to describe the equilibrium constant pressure dependence, allowing to calculate the reaction volumes (Eq. (10)) (Table 1). In addition, using this model, volumetric changes from substrates to products can be evaluated. Positive reaction volumes ( $\Delta V_{\text{Reac}}$ ) of  $18.9 \pm 4.7$  and  $20.0 \pm 5.2$  mL mol $^{-1}$  were obtained, respectively with the substrates 4-NGLuc and 4-NRham. The decrease in hydrolysis equilibrium constants for both 4-NGLuc and 4-NRham as pressure increased (Fig. 3) is in agreement with the positive reaction volumes,  $\Delta V_{\text{Reac}}$ , and to a reaction volume increase. Often volume changes accompanying biochemical reactions are extremely sensitive to the effects of medium and of external factors such as temperature [22].

Assuming that enzyme volume is the same before and after hydrolysis, this result indicates that the system volume increases, when the reaction proceeds from substrate (S) to the products (P). Therefore, as pressure gets higher the equilibrium is directed back to the substrates that occupy together a smaller volume.

#### 4.1.2. Activation volume determination

Experimental values for specific activity of the naringinase enzymatic complex were acquired in the pressure range of 0.1–250 MPa at a temperature of  $40^\circ\text{C}$  (Fig. 4), considering the hydrolysis of 4-NGLuc, 4-NRham and naringin. This flavonoid has both glucose and rhamnose residues that can be hydrolysed by naringinase [10], as well as the residues rhamnose and glucose of 4-Rham and NGLuc, respectively hydrolysed by  $\alpha$ -L-rhamnosidase and  $\beta$ -D-glucosidase.

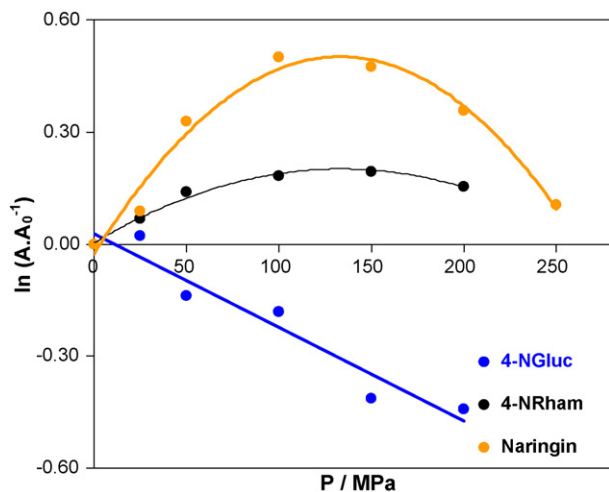


**Fig. 4.** Naringinase specific activity pressure dependence for the hydrolysis of 4-NGLuc, 4-NRham and naringin, in acetate buffer pH = 4.0,  $T=40^\circ\text{C}$  (mean value,  $n=3$ ).

The  $\beta$ -D-glucosidase activity of naringinase decreased with pressures greater than 50 MPa, and at 200 MPa a  $\beta$ -D-glucosidase deactivation of almost 50% was observed (Fig. 4).

Both 4-NRham and naringin hydrolysis rates increased with pressure from 0.1 to 150 MPa. A higher hydrolysis degree occurs on the pressure range of 100–150 MPa, followed by a  $\alpha$ -L-rhamnosidase and naringinase activity decrease. (Fig. 4).

These results are consistent with the distinct effects of the naringinase enzymatic complex towards the different sugars as discriminated by 4-NGLuc and 4-NRham. In reality, naringinase hydrolysis firstly and faster withdraws the rhamnose residue of naringin, as favored by pressure increase, and later and slower the glucose residue, as  $\beta$ -D-glucosidase expression is deactivated by pressure (Fig. 4).

Pressure effects on rate constants ( $k$ ) were quantified according to the best fit of experimental data to first and second order polynomials relating  $\ln k$  to  $P$  or to  $P^2$ , respectively described by the models of Burris and Laidler (Eq. (4)) [16] and Golinkin, Laidlaw and Hyne (Eq. (5)) [17]. These models were used to fit naringinase activity pressure dependence for the substrates, 4-NGLuc, and 4-NRham and naringin, respectively (Table 2).

Pressure affected negatively the reaction rate constant for 4-NGLuc hydrolysis. The experimental results for 4-NGLuc hydrolysis at different pressure were best fitted to the model of Burris and Laidler with a determination coefficient of 0.969. From the slope of  $\ln k$  versus  $P$  an activation volume of  $6.5 \pm 1.9$  mL mol $^{-1}$  was obtained. This positive activation volume means that 4-NGLuc hydrolysis rate was not favoured by a pressure increase.

Regarding the 4-NRham and naringin hydrolysis data were best fitted with model of Golinkin, Laidlaw and Hyne, with a determination coefficient of 0.995 and 0.985, respectively. The  $\Delta V^\ddagger$  values for 4-Rham and naringin hydrolysis, calculated using Eq. (5) are  $-7.7 \pm 1.5$  and  $-20.0 \pm 5.2$  mL mol $^{-1}$ , respectively. These values are related with the initial increase of rate constants on pressure increment.

In previous work the effect of pressure on naringinase activity was tested in different systems [10,23,24]. In fact a positive effect of pressure on reaction rates and a  $\Delta V^\ddagger$  of  $-15.0 \pm 1.8$  mL mol $^{-1}$  were found using soluble naringinase [10]. Moreover a negative  $\Delta V^\ddagger$  ( $-9 \pm 2.8$  mL mol $^{-1}$ ) was obtained with naringinase immobilized in calcium alginate beads [2].

Similar results have been described for the hydrolysis of N,N-dimethylformamide by  $\alpha$ -chymotrypsin, 10 mL mol $^{-1}$  (pressure range 50–450 MPa) [22], as the  $-52$  mL mol $^{-1}$  found for  $\beta$ -galactosidase (pressure range 50–150 MPa) [25], and  $-60$  mL mol $^{-1}$  found for invertase in the pressure range 500–650 MPa [26]. These authors correlate this activation volume changes with conformational alterations and hydration modifications on enzyme and it can represent the hyperbaric stability of the enzyme [26]. In the same pressure range, the more that  $\Delta V^\ddagger$  is negative, the more is the catalytic reaction sensitive to high pressure [25].

The HP induced activation of naringinase making it suitable for substrates processing on optimized naringinase activity whilst

**Table 2**Activation volume estimation, for the hydrolysis of 4-NGLuc, 4-NRham and naringin, by naringinase ( $T=30\text{ }^{\circ}\text{C}$ ) (mean value  $\pm$  standard deviation,  $n=3$ ).

| Substrate                                   | 4-Ngluc                          | 4-Nrham                                 | Naringin                                |
|---|----------------------------------|---|---|
| Fitting model                               | Burriss and Laidler <sup>a</sup> | Golinkin, Laidlaw and Hyne <sup>b</sup> | Golinkin, Laidlaw and Hyne <sup>b</sup> |
| Fitting parameters                          |                                  |   |   |
| A   | $2.63 \times 10^{-2}$            | $3.46 \times 10^{-3}$                   | $2.58 \times 10^{-2}$                   |
| B   | $-2.50 \times 10^{-3}$           | $2.96 \times 10^{-3}$                   | $7.08 \times 10^{-4}$                   |
| C   |                                  | $-1.11 \times 10^{-5}$                  | $-2.98 \times 10^{-5}$                  |
| r   | 0.969                            | 0.995                                   | 0.985                                   |
| F-test                                      |                                  |   |   |
| f   | 0.1                              | 116.9                                   | 114.8                                   |
| f <sub>c</sub>                              | 10.1                             | 10.1                                    | 10.1                                    |
| $\Delta V^{\ddagger}$ /mL mol <sup>-1</sup> | $6.5 \pm 1.9$                    | $-7.7 \pm 1.5$                          | $-20.0 \pm 5.2$                         |

<sup>a</sup>  $\ln k = A + BP$ .<sup>b</sup>  $\ln k = A + BP + CP^2$  (95%).

simultaneously avoiding undesirable pressure labile. Moreover, negative  $\Delta V^{\ddagger}$  values lead us to the hypothesis of accelerating naringinase-catalyzed hydrolysis of naringin by controlling pressure increase.

#### 4.2. Effect of temperature on $\alpha$ -L-rhamnosidase and $\beta$ -D-glucosidase activities of naringinase

The effect of temperature on  $\alpha$ -L-rhamnosidase and  $\beta$ -D-glucosidase activities, expressed by naringinase enzyme complex, was studied individually. Both  $\alpha$ -L-rhamnosidase and  $\beta$ -D-glucosidase activities increased with temperature.

Clearly, the representation of  $\ln$  naringinase specific activity ( $A_{\text{spe}}$ ), for the hydrolysis of 4-NRham, 4-NGLuc and naringin against the absolute temperatures, results in a straight line. Indeed, Arrhenius equation (Eq. (2)) fits well to experimental data (Table 3).

Thermodynamic activation parameters,  $\Delta H^{\ddagger}$ ,  $\Delta S^{\ddagger}$  and  $\Delta G^{\ddagger}$  were evaluated according to Eq. (17)–(19), respectively.

Both hydrolysis of 4-NGLuc and 4-NRham by naringinase were found to be endothermic and endergonic reactions (Table 3).

The Gibbs energy difference between the ground and transition state is related to the rate of reaction and can be considered to be composed of two terms,  $\Delta G_b$ , the binding energy and  $\Delta G_s$ , the activation energy involved in the making and breaking of bonds leading to the transition state. At constant temperature higher rates results in lower standard Gibbs energy of activation ( $\Delta G^{\ddagger}$ ). According to the results depicted in Table 3, the hydrolysis of both 4-NGLuc and 4-NRham occurs faster than the hydrolysis of naringin. This was an expected result as the conversion of naringin to final products takes at least two reaction steps, first to prunin and rhamnose and later to naringenin and glucose. Moreover, the binding energy asso-

ciated with the specific substrate–enzyme interaction is usually a significant factor in lowering the Gibbs energy change required for reaction, being the large bonding energies of substrates due mostly to the complementary shape of the active site of the enzyme. Same trend occurs to activation enthalpy ( $\Delta H^{\ddagger}$ ), in fact it is two and a half times higher in naringin bioconversion. For a bimolecular reaction transition state is formed when the two molecules old bonds are weakened and new bonds begin to form. So, positive and relatively high values for  $\Delta H^{\ddagger}$  occur when covalent bonds are break. Considering the pseudo-equilibrium between reactants, enzyme (E) and substrate (S) stated by TST the formation of the activated complex ( $ES^{\ddagger}$ ), towards the final products (P) and enzymes (E), is easier for the hydrolysis of 4-NRham as it proceeds with a lower activation enthalpy than the hydrolysis of 4-NGLuc. In both reactions the formation of  $ES^{\ddagger}$  occurs with a higher degree of order, as inferred by the negative entropy of activation values [27]. In fact, activation entropy ( $\Delta S^{\ddagger}$ ) will tend to compensate  $\Delta H^{\ddagger}$ . So, the values found for  $\Delta H^{\ddagger}$  on 4-NGLuc and 4-NRham hydrolysis are accompanied with a large decline in entropy from reactants to the transition state, resulting into very negative values,  $-133$  and  $-128 \text{ kJ mol}^{-1} \text{ K}^{-1}$ , respectively.

This agrees with a single step transformation, with a bimolecular reaction mechanism. Opposing to this, in case of naringin hydrolysis, a positive value was found for  $\Delta S^{\ddagger}$  reflecting a mathematical compensation between enthalpy and entropy which does not allow us to infer any assumptions related to structural variations.

The effects of pressure and temperature on the equilibrium or kinetics are antagonistic in molecular terms. As follows from the principle of microscopic ordering, an increase in pressure at constant temperature leads to an ordering of molecules or a decrease in the entropy of the system [6].

**Table 3**Temperature activation parameters for the hydrolysis of 4-NGLuc and 4-NRham by naringinase enzyme complex according to Arrhenius model ( $\ln k = A + B/T$ ) ( $P=0.1 \text{ MPa}$ ).

| Substrate   | 4-NGLuc            | 4-NRham            | Naringin            |
|---|--------------------|--------------------|---------------------|
| Parameters of Arrhenius model                               |                    |                    |                     |
| A   | 14.5               | 15.0               | 39.5                |
| B   | $-5.1 \times 10^3$ | $-5.1 \times 10^3$ | $-12.2 \times 10^3$ |
| Correlation coefficient ( $r^2$ )                           | 0.97               | 0.98               | 0.99                |
| $\Delta H^{\ddagger}$ /kJ mol <sup>-1</sup>                 | $39.8 \pm 9.8$     | $39.6 \pm 8.2$     | $105.2 \pm 3.8$     |
| $\Delta S^{\ddagger}$ /kJ mol <sup>-1</sup> K <sup>-1</sup> | $-133 \pm 32$      | $-128 \pm 27$      | $-46.0 \pm 12.5$    |
| $\Delta G_{293}^{\ddagger}$ /kJ mol <sup>-1</sup>           | 39.0               | 37.7               |                     |
| $\Delta G_{298}^{\ddagger}$ /kJ mol <sup>-1</sup>           | 39.7               | 38.3               | 91.5                |
| $\Delta G_{303}^{\ddagger}$ /kJ mol <sup>-1</sup>           | 40.3               | 39.0               | 91.1                |
| $\Delta G_{308}^{\ddagger}$ /kJ mol <sup>-1</sup>           | 41.0               | 39.6               | 90.9                |
| $\Delta G_{313}^{\ddagger}$ /kJ mol <sup>-1</sup>           | 41.6               | 40.3               | 90.9                |
| $\Delta G_{318}^{\ddagger}$ /kJ mol <sup>-1</sup>           | 42.3               | 40.9               | 91.6                |

Mean value  $\pm$  standard deviation,  $n=3$ .

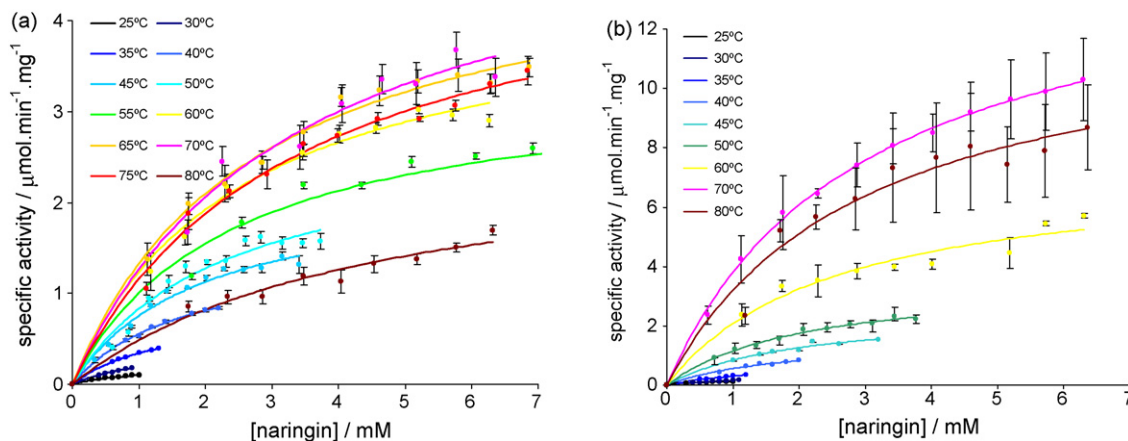


**Fig. 5.** Michaelis–Menten kinetics of naringin hydrolysis by naringinase, at different temperatures (a) under atmospheric (0.1 MPa) and (b) high pressure (150 MPa) conditions (mean value  $\pm$  standard error).

#### 4.3. Effect of pressure and temperature on kinetic parameters of naringinase

Temperature increase and high pressure modulation had been used individually to accelerate enzymatic reactions. In this work we studied the combined effect of high pressure at different temperatures, on naringinase activity of the overall reaction of naringin towards naringenin.

Naringin hydrolysis by naringinase was preformed under atmospheric pressure (0.1 MPa) as well as under high pressure conditions of 150 MPa within a temperature range from 25 to 80 °C (Fig. 5a and b). The range of naringin concentrations increased with the temperatures used. In fact due to naringin solubility limits at lower temperatures (25–35 °C) only a range of 0.2–1 mM concentrations could be used; for temperatures higher than 55 °C, solubility of naringin increased, so a range of 0.2–7 mM naringin concentrations was then used (Fig. 5a and b).

The temperature dependence of Michaelis–Menten constant ( $K_M$ ), catalytic constant ( $k_{cat}$ ) and apparent second-order rate constant ( $k_{cat}/K_M$ ) was achieved in this study (Fig. 5a and b).

The naringinase specific activity increased with temperature till 60 and 70 °C, respectively, at atmospheric (0.1 MPa) and high pressure conditions (150 MPa) (Fig. 5a and b). At atmospheric pressure the rate of naringin hydrolysis diminishes for higher temperatures (>70 °C). A slight increase in  $K_M$  was observed with temperatures from 20 to 60 °C, while for higher temperatures (70 and 80 °C) it almost duplicated, from 2 to 4 mmol L<sup>-1</sup>, at atmospheric pressure.

Under high pressure conditions of 150 MPa, Michaelis–Menten constant remained constant at temperatures from 20 to 50 °C, while for temperatures of 60–80 °C a slight increase was observed, from 2 to 2.5 mM (Fig. 6). A naringin conversion of almost 100% was achieved.

In naringin hydrolysis with naringinase, from *Penicillium* sp., a  $K_M$  of 2 mmol L<sup>-1</sup> was referred, when the enzyme was used

immobilized by covalent binding to wood material [28], while Puri et al. [29] cited a value of 10 mmol L<sup>-1</sup> for the  $K_M$  of naringinase (from *Penicillium* sp.) immobilized in calcium alginate beads. Pedro et al. [2] obtained a  $K_M$  of 0.303 mmol L<sup>-1</sup> and  $V_{max}$  of 0.0418 mmol L<sup>-1</sup> min<sup>-1</sup> with naringinase immobilized in calcium alginate beads in acetate buffer, pH 4 and 30 °C.

An important consequence of pressure application is that the reaction hydrolysis acceleration due to temperature increase is more significant under higher pressure conditions. The catalytic constant, as well as, the apparent second-order rate constant showed an increase till the temperature of 70 °C was reached, where the enzyme activity is highest, decreasing afterwards. Around this temperature both the catalytic constant and apparent second-order rate constant showed higher values, respectively 15 mmol min<sup>-1</sup> mg<sup>-1</sup> and 5 L min<sup>-1</sup> g<sup>-1</sup> under high pressure than at atmospheric pressure, respectively 5 mmol min<sup>-1</sup> mg<sup>-1</sup> and 1.5 L min<sup>-1</sup> g<sup>-1</sup> (Fig. 5a and b). The  $k_{cat}$  and  $k_{cat}/K_M$  for the naringinase-catalyzed hydrolysis of naringin is not only temperature dependent but pressure as well. Under high pressure, at 70 °C  $k_{cat}$  and  $k_{cat}/K_M$  are 3-fold higher than at atmospheric pressure (Fig. 7a and b) and is even higher at 80 °C, more than 4-fold (Fig. 7a). When these values are compared at 30 °C a 15-fold increase is observed at 70 °C under 150 MPa. Similar results were obtained with  $\alpha$ -chymotrypsin [22], at 50 °C and 360 MPa, with an activity more than 30-fold higher than the activity determined at atmospheric pressure and 20 °C [22]. These authors assumed that activation volumes values increase with a temperature increase, so the effect of increasing pressure effects on reaction rates by temperature could have realistic use for accelerating enzymatic reactions [22].

This stated pressure dependence is in agreement with a pressure stabilization of protein, underlying a positive pressure effect on naringinase native state at higher temperatures

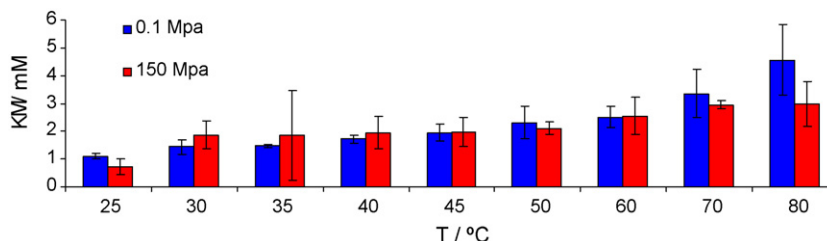


**Fig. 6.** Michaelis–Menten constant temperature dependence under atmospheric (0.1 MPa) and high pressure (150 MPa) (mean value  $\pm$  standard error).

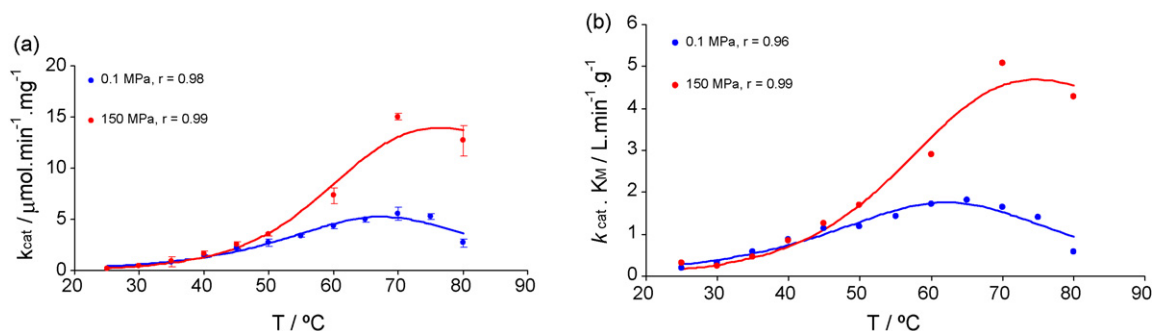


**Fig. 7.** (a) Catalytic constant ( $k_{cat}$ ) and (b) second-order constant ( $k_{cat}/K_M$ ) temperature dependence under atmospheric (0.1 MPa) and high pressure (150 MPa) (mean value  $\pm$  standard error).

## 5. Conclusion

Pressure effects on equilibrium constants were quantified according to the fit of experimental data to Baliga and Whalley model. Positive reaction volumes ( $\Delta V_{\text{Reac}}$ ) of 64.3 and 93.1  $\text{mL}\cdot\text{mol}^{-1}$  were obtained, respectively with the substrates 4-NGLuc and 4-NRham. The decrease in hydrolysis equilibrium constants for both 4-NGLuc and 4-NRham as pressure increased (Fig. 3) is in agreement with the positive reaction volumes,  $\Delta V_{\text{Reac}}$ , and to a reaction volume increase.

Pressure effects on rate constants ( $k$ ) were quantified according to the best fit of experimental data to the models of Burris and Laidler (Eq. (4)) and Golinkin, Laidlaw and Hyne (Eq. (5)). The  $\Delta V^{\ddagger}$  values for 4-Rham and naringin hydrolysis, calculated using Eq. (5) are  $-7.7 \pm 1.5$  and  $-20.0 \pm 5.2$   $\text{mL}\cdot\text{mol}^{-1}$ , respectively, which is in agreement with the increase of rate constants on pressure increment.

Moreover, negative  $\Delta V^{\ddagger}$  values lead us to the hypothesis of accelerating naringinase-catalyzed hydrolysis of 4-Rham and naringin by controlling pressure increase.

The catalytic constant as well as the apparent second-order rate for the naringinase-catalyzed hydrolysis of naringin is not only temperature dependent but pressure as well. Under high pressure, at 70  $^{\circ}\text{C}$  the apparent second-order rate is 3-fold higher than atmospheric pressure and is even higher at 80  $^{\circ}\text{C}$ , 4-fold. This stated pressure dependence is in agreement with pressure stabilization of the enzyme native state, at high temperatures. In conclusion the effect of amplification of pressure effects on reaction rates by temperature could have a pragmatic use for accelerating enzymatic reactions.

## Acknowledgement

Helder Vila Real is grateful to FCT for the financial support of his Ph.D. Grant (SFRH/BD/30716/2006).

## References

- [1] J.D. Pollard, J.M. Woodley, Trends Biotechnol. 25 (2007) 66–73.
- [2] H.A.L. Pedro, A.J. Alfaia, J. Marques, H.J. Vila-Real, A. Calado, M.H.L. Ribeiro, Enzyme Microb. Technol. 40 (2007) 442–446.
- [3] S. Hay, M.J. Sutcliffe, N.S. Scrutton, Proc. Natl. Acad. Sci. 9 (2007) 507–512.
- [4] M.J. Eisenmenger, J.I. Reyes-De-Corcuera, Enzyme Microb. Technol. 45 (2009) 118–125.
- [5] V. Lullien-Pellerin, C. Balny, Inn. Food Sci. Emerg. Technol. 3 (2002) 209–221.
- [6] C. Balny, J. Phys. Condens. Matter 16 (2004) S1245–S1253.
- [7] D.B. Northrop, Biochim. Biophys. Acta 1595 (2002) 71–79.
- [8] C.T. Scharnagl, M. Reif, J. Friedrich, Biochim. Biophys. Acta (2005) 187–213.
- [9] K. Heremans, L. Smeller, Biochim. Biophys. Acta 1386 (1998) 353–370.
- [10] H.J. Vila Real, A.J. Alfaia, A.R.T. Calado, M.H.L. Ribeiro, Food Chem. 102 (2007) 565–570.
- [11] I.A. Ribeiro, J. Rocha, B. Sepodes, H. Mota-Filipe, M.H.L. Ribeiro, J. Mol. Catal. B: Enzyme 52 (2008) 13–18.
- [12] M.I. Amaro, J. Rocha, H. Vila-Real, M.E. Figueira, H. Mota-Filipe, B. Sepodes, M.H. Ribeiro, Food Res. Int. 42 (2009) 1010–1017.
- [13] D.G. Truhlar, B.C. Garrett, S.J. Klippenstein, J. Phys. Chem. 100 (1996) 12771–12800.
- [14] D. Mamma, E. Kalogeris, D.G. Hatzinikolaou, A. Lekanidou, D. Kekos, B.J. Macris, P. Christakopoulos, Food Biotechnol. 18 (2004) 1–18.
- [15] S. Wold, P. Ahlberg, Acta Chem. Scand. 24 (1970) 618–632.
- [16] C.T. Burris, K.J. Laidler, Trans. Faraday Soc. 51 (1955) 1497–1505.
- [17] H.S. Golinkin, W.G. Laidlaw, J.B. Hyne, Can. J. Chem. 44 (1966) 2193–2203.
- [18] B.T. Baliga, E. Whalley, Can. J. Chem. 48 (1970) 528–536.
- [19] C. Walling, D.D. Tanner, J. Am. Chem. Soc. 85 (1963) 612–615.
- [20] G.L. Miller, Anal. Chem. 31 (1959) 426–428.
- [21] M. Bradford, Anal. Biochem. 72 (1976) 248–254.
- [22] V.V. Mozhaev, K. Heremans, J. Frank, P. Mansson, C. Balny, Protein Struct. Funct. Genet. 24 (1996) 81–91.
- [23] J. Marques, H.J. Vila-Real, A.J. Alfaia, M.H.L. Ribeiro, Food Chem. 105 (2007) 504–510.
- [24] M.H.L. Ribeiro, C. Afonso, H.J. Vila-Real, A.J. Alfaia, L. Ferreira, LWT—Food Sci. Technol. 43 (2010) 482–487.
- [25] D. Cavaillé-Lefebvre, D. Combes, J. Biotechnol. 61 (1998) 85–93.
- [26] D. Cavaillé, D. Combes, J. Biotechnol. 43 (1995) 221–228.
- [27] T. Lonhienne, C. Gerday, G. Feller, Biochim. Biophys. Acta (BBA)—Protein Struct. Mol. Enzymol. 1543 (2000) 1–10.
- [28] M. Puri, H. Kaur, J.F. Kennedy, J. Chem. Technol. Biotechnol. 80 (2005) 1160.
- [29] M. Puri, S.S. Marwaha, R.M. Kothari, Enzyme Microb. Technol. 18 (1996) 281.